ELSEVIER

Journal of Biomechanics 38 (2005) 529–535

JOURNAL OF BIOMECHANICS

www.elsevier.com/locate/jbiomech
www.JBiomech.com

Cell relaxation after electrodeformation: effect of latrunculin A on cytoskeletal actin

Pak Kin Wong[a], Winny Tan[b], Chih-Ming Ho[a,*]

[a] Department of Mechanical and Aerospace Engineering, University of California, Los Angeles, CA 90095, USA
[b] Department of Biomedical Engineering, University of California, Los Angeles, CA 90095, USA

Accepted 4 April 2004

Abstract

Precise measurement of the mechanical properties of a cell provides useful information about its structural organization and physiological state. It is interesting to understand the effect of individual components on the mechanical properties of the entire cell. In this study, we investigate the influence of the cytoskeletal actin on the viscoelastic properties of a cell. Actin-specific agents, including latrunculin A and jasplakinolide, are used to alter the organization of the cytoskeletal actin. *Brassica oleracea* protoplasts are treated with the drugs and deformed under an external electric potential. The relaxation processes of single protoplasts after electrodeformation are measured. The data are analyzed by a model-independent spectrum recovery algorithm. Two distinct characteristic time constants are obtained from the relaxation spectra. Treatment with latrunculin A increases both of the relaxation time constants. The longest relaxation times for control, latrunculin A treated, and jasplakinolide treated cells are determined to be 0.28, 1.0, and 0.21 s, respectively.

Keywords: Cytoskeleton; Latrunculin A; Actin; Electrodeformation; Cell relaxation

1. Introduction

Direct measurement of the mechanical properties of a cell is a powerful tool in the study of cellular structures and their functions (Elson, 1988). The viscoelastic properties are related to the physiological state of a cell and it reflects changes due to disease, environmental stimulation, or metabolic defects. For example, the deformability of red blood cells can distinguish young cells from aged cells and can be directly applied in the diagnosis of many diseases, such as sickle cell anemia and elliptocytosis (Mokken et al., 1992; Dobbe et al., 2002).

Several methods have been reported for measuring cell deformability, including rheoscope (Dobbe et al., 2002), centrifugation (Mege et al., 1985), cell poker (McConnaughey and Petersen, 1980), and atomic force microscope (A-Hassan et al., 1988). Among the methods, micropipette aspiration (Mitchison and Swann, 1954) and optical trapping (Ashkin and Dziedzic, 1987) are the most frequently applied techniques for measuring the elastic properties of single cells (Hochmuth, 2000; Bronkhorst et al., 1995). Measurement with micropipette aspiration, however, is sensitive to the pipette dimensions. In addition, long exposure to a laser beam necessary for optical trapping can induce morphological changes and decrease the deformability of the cell (Bronkhorst et al., 1995; Kaneta et al., 2001). Moreover, both micropipette and laser trapping are relatively labor intensive and time consuming.

With the recent advancement of micromachining technology, synthetic microchannel arrays of defined geometry can be fabricated (Brody et al., 1995; Gifford et al., 2003). Similar to micropipette aspiration, cells are deformed once they enter into the microchannel and their mechanical properties can be studied. In addition, a cell can be deformed by an external electric field (Friend et al., 1975). Electrodeformation using

*Corresponding author. Tel.: +1-310-825-9993; fax: +1-310-206-2302.
E-mail address: chihming@ucla.edu (C.-M. Ho).

0021-9290/$ - see front matter © 2004 Elsevier Ltd. All rights reserved.
doi:10.1016/j.jbiomech.2004.04.008

microelectrode arrays is an attractive choice for studying single cell deformability. With MEMS technology, fabrication of well-defined electrode arrays is a relatively straightforward task and electrokinetic forces are especially effective in the micro scale (Wong et al., 2003). Information obtained from electrokinetic measurements, such as frequency-dependent phenomena, provides insightful information about cellular structures and their properties (Jones, 1995). Furthermore, the parallel processing nature of the techniques allows for analysis of a large number of cells under different experimental conditions.

In general, the viscoelastic properties of a cell are the combined effects of several cellular components, including the lipid/protein bilayer, the cytoskeleton, the organelles, and the cytosol. It is important to understand the mechanical properties of the components and their influences to the overall viscoelastic response. Different approaches have been applied to study the influence of individual cellular components, such as cross-linked surface receptors (Pasternak and Elson, 1985), gene expression (Yao et al., 2002), and the plasma membrane (Morimoto et al., 2002). Of special importance is the cytoskeleton, which has been shown to be responsible for various important mechanical functions.

Cytochalasin, a family of cytoskeletal poisons, was commonly used in the early studies of cytoskeletal actin (Peterson and Mitchison, 2002). It is known that cytochalasin can disturb the dynamics of the rapidly growing end of actin filaments and alter the organization of the cytoskeletal actin. Reduction in cell deformability after treatment of cytochalasin has been characterized by different methods (Tsai et al., 1994; Ting-Beall et al., 1995; Pawlowski et al., 1997). There is no doubt that cytochalasin is invaluable for studying the function of the cytoskeletal actin, such as motility, ruffling and cytokinesis (Peterson and Mitchison, 2002). However, the detailed molecular effects of cytochalasin are not fully understood (Cooper, 1987; Baluška et al., 2001). Polymerization of actin filaments (Foissner and Wasteneys, 1997) and the formation of short rods (Collings et al., 1995) have also been reported. Furthermore, cytochalasin B was shown to inhibit glucose uptake by the cells (Kletzien and Perdue, 1973). It is valuable to perform a cell deformability study using actin-specific agents with well-understood molecular effects. Useful information of the cytoskeletal actin can be obtained to improve our understanding in cell mechanics.

In this study, we investigate the effect of latrunculin A on cytoskeletal actin. The deformability of *Brassica oleracea* (cabbage) protoplasts is studied by electrodeformation. Any future theoretical analysis will be simplified due to the protoplast's spherical shape and simple structure. The electric field strength and frequency dependence of electrodeformation for the protoplasts are measured. The viscoelastic properties are measured for protoplasts treated with latrunculin A, an actin filament-disrupting agent. It has been shown that latrunculin A is a more potent actin inhibitor compared to cytochalasin (Spector et al., 1989). Moreover, latrunculin has relatively well understood mode of action (Baluška et al., 2001). The specific and well-understood mode of action of latrunculin A is advantageous in the study of the mechanical properties of cytoskeletal actin (Yarmola et al., 2000). In addition, we also study the effects of jasplakinolide, an actin-stabilizing agent, to the viscoelastic properties of the protoplasts. The results of electrodeformation and relaxation of the cells after different drug treatments are compared and discussed.

2. Materials and methods

The microelectrodes for electrodeformation were fabricated on a glass substrate. A 3000 Å thick gold layer with a 200 Å thick chromium adhesion layer was evaporated on the microscope slide and patterned by lift-off. The electrode design consisted of a central electrode surrounded by an outer electrode. The diameter of the central electrode was 200 μm and the gap distance between the electrodes was 220 μm. Spacers of 125 μm were placed on the chip to define the height of the fluid chamber. The chip was covered by a cover slip during the experiment. The chip was observed with an epi-fluorescence microscope (Nikon, TE200) equipped with a 100 W mercury lamp. A function generator (HP, 33120A) was used to provide the AC signal for electrodeformation. The cell dynamics were recorded by a CCD camera (Panasonic, GP-KR222) and directly digitized by a video capture system (Pinnacle, PCTV). The digitized images were then analyzed with a computer program to extract cell deformation information. Fluorescence images were captured by a 1024×1024 pixel, 16-bit cooled CCD camera (Photometric, CH350L).

B. oleracea protoplasts were used in the experiment. The cell wall of fresh cabbage tissue was enzymatically digested with 2% cellulase (Sigma, C-1794) and 0.3% pectinase (Sigma, P-2401) in an isotonic medium containing 500 mM D-Sorbitol, 1 mM $CaCl_2$, and 5 mM MES. After incubation with the enzymes for 3 h at room temperature, the cells were washed out with the same medium. The pH value of the wash medium was adjusted to 6 with addition of KOH. The conductivity of the medium was 0.34 mS/cm. Cells were incubated with 10 μM jasplakinolide (Molecular Probes, J7473) and 10 μM latrunculin A (Molecular Probes, L12370) at 4°C for 2 h prior to the stretch-and-relax experiment. Jasplakinolide (1.4 mM) and latrunculin A (2.37 mM) stock solutions were prepared in DMSO and diluted

with the wash medium to the appropriate working solution. All the experiments were performed at room temperature (22–24°C).

For fluorescence measurement, the cells were fixed with 2% formaldehyde at 4°C for 1 h. The sample was centrifuged to remove the supernatant. The pellet was then resuspended in the wash medium with 0.2% Tween 20. The mixture was incubated in a 37°C water bath for 15 min. After removing the supernatant and resuspending in the wash medium, Alexa Fluor 488 phalloidin (300 unit/ml, Molecular probes, A12379) was added into the solution to specifically label the actin filaments. The solution was allowed to equilibrate for more than 30 min before performing the observation.

To perform the stretch-and-relax experiment, we first applied an AC voltage of ~3 V (peak voltage) at 1 MHz to capture the suspended cells to the electrode edge. At the given experimental condition, the cells displayed positive dielectrophoresis and were attracted to the electrode edges. The cells were at rest in equilibrium before performing the experiment. Various voltages and frequencies were applied to study the response of the cell under an external electric field. For relaxation measurements, the cells were stretched to have a deformation of approximately 15% of its original length along the direction of the electric field. Then, the electric field was suddenly removed and the relaxation process of the cell was recorded and analyzed.

An inverse Laplace transform algorithm was developed to analyze the relaxation response. The relaxation data can be represented by an integral over an effectively continuous spectrum of exponential functions.

$$L(t) = \int_{\tau_{\min}}^{\tau_{\max}} x(\tau) e^{-t/\tau}\, d\tau + L_0 + \beta, \tag{1}$$

where $L(t)$ is the length, τ is the relaxation time, $x(\tau)$ is the spectrum of the exponential functions, L_0 is the length of the cell at equilibrium, and β is an unknown noise component. The problem is well known to be ill-posed and the solution is extremely sensitive to noise (Provencher and Dovi, 1979). A common strategy for solving the problem is to reduce the number of degrees of freedom (e.g. fitting the data with a parameterized model). It is obviously interesting to estimate $x(\tau)$ directly from the data. Instead of directly solving the inverse problem, we considered the following penalized least squares minimization problem (Provencher, 1982):

$$\min_{x\geqslant 0} f(x) = \min_{x\geqslant 0} \frac{1}{2}|L - L_0 - Ax|^2 + \alpha J(x), \tag{2}$$

where x is a vector representing the amplitude of the relaxation spectrum, L is the vector of the relaxation data, A is the discrete version of the integral of exponential functions in matrix form, $\alpha \geqslant 0$ is the regularization parameter, and $J(x)$ is the square of the Sobolev H-1 penalty. The relaxation spectrum x was constrained to be nonnegative. The constrained minimization problem can be solved numerically by using the projected Newton method (Bertsekas, 1982). In the calculation, the upper and lower limits of relaxation time ($\tau_{\max}$ and $\tau_{\min}$) considered were 100 and 0.01 s, respectively. A process with relaxation time longer than 100 s would decay less than 1% in 1 s, which is indistinguishable in our measurement. A process with relaxation time shorter than 0.01 s is difficult to be measured with our recording system (30 frames/s).

3. Results

Deformations of the protoplasts at different frequencies were measured. The electric field strength was kept constant (136 V^{-1}cm). The length of the cell was normalized by the undeformed length. Electrodeformation shows bell-shaped frequency dependence (Fig. 1). The deformation increases with the applied frequency at 100 kHz. The deformation reaches its maximum value at roughly 2 MHz. The deformation is approximately constant in frequencies between 2 and 5 MHz. The cell deformation decreases when the frequency is further increased (> 5 MHz).

We have also measured the electric field dependence of cell deformation (Fig. 2). The frequency of the AC electric field was 1 MHz. The deformation data was fitted by the method of least squares to the function:

$$L(E) = K_E E^{\alpha} + L_0, \tag{3}$$

where K_E is a constant, E is the electric field strength, and α is the exponent of electric field dependence. α was determined to be 1.6. Diversity in cell deformability was observed as indicated by the error bar (Fig. 2). Under small deformation (less than 30% of the original length), the deformation of the cell is reversible. No change in cell morphology or mechanical properties was observed. If the electric field is further increased (larger than

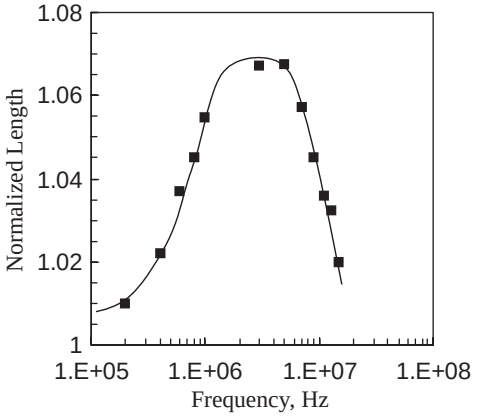

Fig. 1. Frequency dependence of electrodeformation. The electric field strength was 136 V/cm.

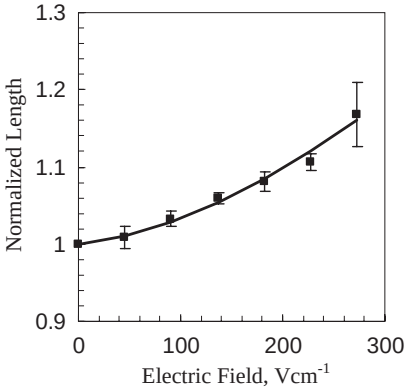

Fig. 2. Electric field dependence of electrodeformation. The solid symbols and bars indicate average values and standard deviations obtained from 8 cells. The frequency of the AC electric field was 1 MHz. Solid line represents the least square fit of the data.

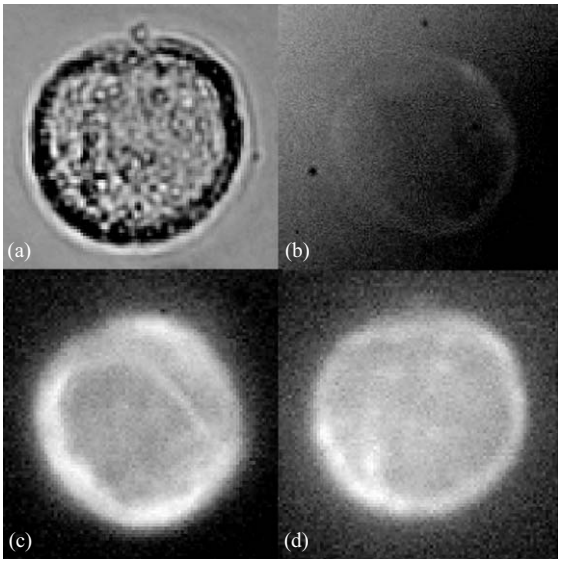

Fig. 3. Phase contrast image (a) and fluorescence images of latrunculin A treated (b), control (c) and jasplakinolide treated (d) cells. Cells were fixed and stained with Alexa Fluor 488 conjugated with phalloidin. The cells are approximately 40 μm in diameter.

400 V^{-1}/cm), irreversible (plastic) deformation and cell membrane rupturing are observed.

There was no observable morphology change of the cells after the drug treatments. Fluorescence microscopy was used to investigate the effects of the drugs to the cytoskeletal actin (Fig. 3). Fluorescence images indicate that actin filament is almost absent after treatment of latrunculin A. Treatment of jasplakinolide shows minimal effect on the cytoskeleton as shown in the fluorescence images. The deformability of the cells increases significantly after treatment of latrunculin A while the effect of jasplakinolide on the deformability is small. At an electric field strength of 180 V cm^{-1}, the deformation of the latrunculin A treated, control, and

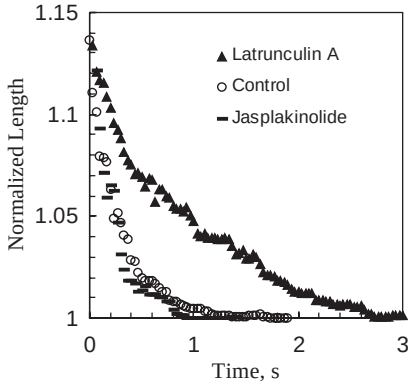

Fig. 4. Relaxations of latrunculin A treated, jasplakinolide treated and control cells. Each curve represents average of at least 9 relaxation measurements.

jasplakinolide treated cells are 16%, 8%, and 9% of the undeformed length, respectively.

Relaxation data of individual cells were normalized by the undeformed lengths. It was found that the curves can collapse into a single relaxation curve. The relaxation curves for cells treated with different drugs are compared (Fig. 4). Each curve represents at least nine relaxation measurements of individual cells. A significant change of the viscoelastic response was observed for latrunculin A treated cells. We used two different methods to analyze the data. In the first method, the last portions of the relaxation curves (less than 0.1 of the undeformed length) are fitted using the method of least squares to a single exponential function:

$$L(t) = K_R e^{-t/\tau} + L_0, \tag{4}$$

where K_R is a constant. The relaxation time τ can then be extracted form the data. The relaxation times were determined to be 0.89, 0.31 and 0.20 s for latrunculin A treated, control, and jasplakinolide treated cells, respectively. In the second method, we analyzed the data with the inverse Laplace transform algorithm. Two discrete peaks were observed in the relaxation spectra (Fig. 5). The amplitudes are larger for the peaks corresponding to the longest relaxation times. The longest relaxation times determined by the peak positions are 1.0, 0.28 and 0.21 s for latrunculin A treated, control, and jasplakinolide treated cells, respectively.

4. Discussion

Under small deformation, the elastic strain of a cell is given by (Engelhardt and Sackmann, 1988; Sukhorukov et al., 1998)

$$\frac{L - L_0}{L_0} = K_S E^2 \mathrm{Re}(U(\omega)), \tag{5}$$

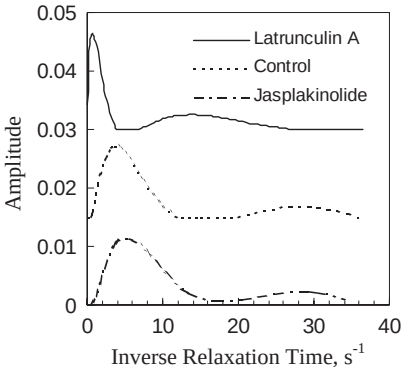

Fig. 5. The spectra of decaying exponentials for latrunculin A treated, control and jasplakinolide treated cells determined by an inverse Laplace transformation of the relaxation data. The spectrum for the control cell and latrunculin A are shifted up by 0.015 and 0.03 for clarity.

where K_S is a constant reflecting the elastic properties of the protoplast, ω is the angular frequency of the AC electric field, and $U(\omega)$ is the complex Clausius–Mossotti function. The frequency dependence of electrodeformation (and dielectrophoresis) is given by the real part of the complex Clausius–Mossotti function $U(\omega)$. The Clausius–Mossotti factor can be estimated by modeling a protoplast to be a conductive fluid interior enclosed by a thin layer of insulating membrane. The membrane is assumed to have a membrane capacitance c_m and negligible conductance. The Clausius–Mossotti factor for a protoplast with radius R is given by (Jones, 1995)

$$U(\omega) = -\frac{\omega^2(\tau_e\tau_{mc} - \tau_c\tau_{me}) + j\omega(\tau_{me} - \tau_e - \tau_{mc}) - 1}{\omega^2(\tau_c\tau_{me} + 2\tau_e\tau_{mc}) - j\omega(\tau_{me} + 2\tau_e + \tau_{mc}) - 2}, \quad (6)$$

where $\tau_{me} = c_m R/\sigma_e$, $\tau_{mc} = c_m R/\sigma_c$, $\tau_e = \varepsilon_e/\sigma_e$, $\tau_c = \varepsilon_c/\sigma_c$. ε and σ are the permittivity and conductivity. The subscript c and e indicate the cytosol and the external medium. τ_c and τ_e are the charge relaxation time for the cytosol and the external medium. τ_{me} and τ_{mc} are the membrane charging times constant.

The model describes three distinctive mechanisms of the polarization in different frequency ranges. At low frequency (small compared to the inverse of the membrane charging time), the cell membrane behaves as insulator and the induced dipole is dominated by the free charges that accumulate at the interfaces of the cell membrane. The Clauisus–Mossotti factor is approximately -0.5. At intermediate frequencies, the membrane impedance is low and the response is dominated by the conductivity of the cytosol and external medium. The Clausius–Mossotti factor can be estimated by $(\sigma_c - \sigma_e)/(\sigma_c + 2\sigma_e)$. At high frequency (larger than the inverse of the charge relaxation time), the charges cannot respond to the fast changing electric field and the protoplast behaves as a homogeneous dielectric sphere. The Clausius–Mossotti factor can be simplified to $(\varepsilon_c - \varepsilon_e)/(\varepsilon_c + 2\varepsilon_e)$. Our data are in good agreement with the model. Consider the membrane capacitance to be $1\,\mu F/cm^2$, the membrane changing time is approximately in the order of $10\,\mu s$ (Zimmermann, 1982). It is consistence with our observation that there is an increase of cell deformation observed in the range of 100 kHz. The charge relaxation is responsible for the decrease of strain observed in a few megahertz. The charge relaxation time is calculated to be in the order of nanosecond for cytoplasmic conductivity of 5 ms/cm (Jones, 1995).

In our measurement, the exponential for electric field dependence is determined to be 1.6, which is smaller than the quadratic dependence predicted in Eq. (5). Nevertheless, our measurement is consistent with the observation for human erythrocytes at large deformation (for strain larger than 0.4) (Zimmermann et al., 2000). The deviation occurs at much smaller strain in our experiment (strain less than 0.2). The difference is likely due to the intrinsic mechanical properties of the cells. It should be noted that the membrane of the *B. oleracea* protoplast ruptures at a strain of roughly 0.5 while the erythrocytes could be reversibly deformed at a strain up to 0.7 (Sukhorukov et al., 1998; Zimmermann et al., 2000). Moreover, it should be noted that control and jasplakinolide treated cells show actin patching (Fig. 3c and d). The heterogeneity of actin distribution may contribute to the diversity of the cell deformability and account for deviation from quadratic behavior. Electrical effects should also be taken into consideration. The non-uniformity of the electric field near the electrode edge can play a role to the electric field dependence. The theoretical analysis of electrodeformation is restricted to uniform electric field and small deformation. However, there is actually a strong electric field gradient near the electrode. The electric field gradient is responsible for the dielectrophoretic capturing of the protoplasts to the electrode edge.

The characteristic relaxation time is determined by the ratio of the viscous damping and the cell elasticity. As indicated in fluorescence measurement, latrunculin A is able to disturb the cytoskeletal actin. The change in elasticity of the cells can be determined from the electrodeformation data. The deformation of the cells increases by a factor of ~ 2 after treatment with latrunculin A. It is in agreement with the finding of neutrophils with cytochalasin (Tsai et al., 1994; Ting-Beall et al., 1995). On the other hand, we also measured the relaxation times of the cells after electrodeformation. After the treatment with latrunculin A, the characteristic time increases for a factor ~ 3 while the deformability of the cell increase by a factor of ~ 2. Therefore, the measurements indicate that the treatment of latrunculin A increases the viscous damping roughly 50%. It has

been shown that the energy dissipated by the cytoplasm and the outside medium is small and that the viscous damping is dominated by the membrane viscosity (Hochmuth et al., 1979). The increase in relaxation time is due to a decrease in the elastic restoring force as well as to an increase in the membrane viscosity. Further study is required to investigate the molecular origin of the increase in the membrane viscosity.

The spectrum recovery algorithm allows data analysis that is independent of the model. Two distinct relaxation times, separated by a factor of ~ 8, are observed in the relaxation spectrum of the control cells. Relatively small changes in the relaxation times are observed for cells treated with jasplakinolide. After treatment with latrunculin A, both relaxation times increase and they are separated by a factor of ~ 14. Our findings are in qualitative agreement with other researchers. It has been reported that the relaxation of leukocytes show an initial rapid coiling followed by a slower asymptotic recovery (Sung et al., 1988). The relaxation data from erythrocyte and *Neurospora crassa* can be fitted into a bi-exponential function and the two time constants are different by a factor of 10–20 (Engelhardt and Sackmann, 1988; Poznański et al., 1992; Pawlowski et al., 1997). The quantitative difference can be explained by the intrinsic difference of the cellular structures and the methods used in the data analysis. Currently, there is no existing theory can quantitatively describe all the observations from different cells with different structures. Our measurement, combined with data from other researchers, can contribute to further development of microscopic theories for cell mechanics.

Acknowledgements

This work is supported by CMISE through NASA URETI program. The authors would like to thank Ming-Ham Yip for his valuable suggestions in the development of the algorithm for the relaxation spectrum analysis.

References

A-Hassan, E., Heinz, W.F., Antonik, M.D., D'Costa, N.P., Nageswaran, S., Schoenenberger, C.-A., Hoh, J.H., 1988. Relative microelastic mapping living cells by atomic force microscopy. Biophysical Journal 74, 1564–1578.

Ashkin, A., Dziedzic, J.M., 1987. Optical trapping and manipulation of viruses and bacteria. Science 235, 1517–1520.

Baluška, F., Jasik, J., Edelmann, H.G., Salajova, T., Volkmann, D., 2001. Latrunculin B-induced plant dwarfism: plant cell elongation is f-actin-dependent. Developmental Biology 231, 113–124.

Bertsekas, D., 1982. Projected Newton methods for optimization problems with simple constraints. SIAM Journal of Control and Optimization 20, 221–246.

Brody, J.P., Han, Y., Austin, R.H., Bitensky, M., 1995. Deformation and flow of red blood cells in a synthetic lattice: evidence for an active cytoskeleton. Biophysical Journal 68, 2224–2232.

Bronkhorst, P.J.H., Streekstra, G.J., Grimbergen, J., Nijhof, E.J., Sixma, J.J., Brakenhoff, G.J., 1995. A new method to study shape recovery of red blood cells using multiple optical trapping. Biophysical Journal 69, 1666–1673.

Collings, D.A., Wasteneys, G.O., Willamson, R.E., 1995. Cytochalasin rearranges cortical actin of the alga Nitella into short, stable rods. Plant and Cell Physiology 36, 765–772.

Cooper, J.A., 1987. Effect of cytochalasin and phalloidin on actin. The Journal of Cell Biology 105, 1473–1478.

Dobbe, J.G.G., Streekstra, G.J., Hardeman, M.R., Ince, C., Grimbergen, C.A., 2002. Measurement of the distribution of red blood cell deformability using an automated rheoscope. Cytometry 50, 313–325.

Elson, E.L., 1988. Cellular mechanics as an indicator of cytoskeleton structure and function. Annual Review of Biophysics and Biophysical Chemistry 17, 397–430.

Engelhardt, H., Sackmann, E., 1988. On the measurement of shear elastic moduli and viscosities of erythrocyte plasma membranes by transient deformation in high frequency electric fields. Biophysical Journal 54, 495–508.

Foissner, I., Wasteneys, G.O., 1997. A cytochalasin-sensitive actin filament meshwork is a prerequisite for local wound wall deposition in *Nitella* internodal cells. Protoplasma 200, 17–30.

Friend, A.W., Finch, E.D., Schwan, H.P., 1975. Low-frequency electric-field induced changes in shape and motility of amoebas. Science 187, 357–359.

Gifford, S.C., Frank, M.G., Derganc, J., Gabel, C., Austin, R.H., Yoshida, T., Bitensky, M.W., 2003. Parallel microchannel-based measurements of individual erythrocyte areas and volume. Biophysical Journal 84, 623–633.

Hochmuth, R.M., 2000. Micropipette aspiration of living cells. Journal of Biomechanics 33, 15–22.

Hochmuth, R.M., Worthy, P.R., Evans, E.A., 1979. Red cell extensional recovery and the determination of membrane viscosity. Biophysical Journal 26, 101–114.

Jones, T.B., 1995. Electromechanics of Particles. Cambridge University Press, New York.

Kaneta, T., Makihara, J., Imasaka, T., 2001. An Optical Channel: a technique for the evaluation of biology cell elasticity. Analytical Chemistry 73, 5791–5795.

Kletzien, R.F., Perdue, J.F., 1973. The inhibition of sugar transport in chick embryo fibroblasts by cytochalasin B. Evidence for a membrane-specific effect. The Journal of Biological Chemistry 248, 711–719.

McConnaughey, W.B., Petersen, N.O., 1980. Cell poker—an apparatus for stress–strain measurements on living cells. Review of Scientific Instrument 51, 575–580.

Mege, J.L., Capo, C., Benoliel, A.M., Foa, C., Bongrand, P., 1985. Study of cell deformability by a simple method. Journal of Immunological Methods 82, 3–15.

Mitchison, J.M., Swann, M.M., 1954. The mechanical properties of the cell surface: I. the cell elastimeter. Journal of Experimental Biology 31, 443–460.

Mokken, F.Ch., Kedaria, M., Henny, Ch.P., Hardeman, M.R., Gelb, A.W., 1992. The clinical importance of erythrocyte deformability, a hemorrheological parameter. Annals of Hematology 64, 113–122.

Morimoto, N., Raphael, R.M., Nygren, A., Brownell, W.E., 2002. Excess plasma membrane and effects of ionic amphipaths on mechanics of outer hair cell lateral wall. American Journal of Physiology—Cell Physiology 282, C1076–1086.

Pasternak, C., Elson, E.L., 1985. Lymphocyte mechanical response triggered by cross-linking surface receptors. The Journal of Cell Biology 100, 860–872.

Pawlowski, P., Poznanska, A., Fikus, M., 1997. Bioelectrorheological model of the cell. 7. Cellular deformation in the presence of cytochalasin B. Biorheology 34, 171–193.

Peterson, J.R., Mitchison, T.J., 2002. Small molecules, big impact: a history of chemical inhibitors and the cytoskeleton. Chemistry and Biology 9, 1275–1285.

Poznański, J., Pawłowski, P., Fikus, M., 1992. Bioelectrorheological model of the cell. 3. Viscoelastic shear deformation of the membrane. Biophysical Journal 61, 612–620.

Provencher, S.W., 1982. A constrained regularization method for inverting data represented by linear algebraic or integral equations. Computer Physics Communications 27, 213–227.

Provencher, S.W., Dovi, V.G., 1979. Direct analysis of continuous relaxation spectra. Journal of Biochemical and Biophysical Methods 1, 313–318.

Spector, I., Shochet, N.R., Blasberger, D., Kashman, Y., 1989. Latrunculins—novel marine macrolides that disrupt microfilament organization and affect cell growth: I. comparison with cytochalasin d. Cell Motility and the Cytoskeleton 13, 127–144.

Sukhorukov, V.L., Mussauer, H., Zimmermann, U., 1998. The effect of electrical deformation forces on the electropermeabilization of erythrocyte membranes in low- and high-conductivity media. The Journal of Membrane Biology 163, 235–245.

Sung, K.-L.P., Dong, C., Schmid-Schönbein, G.W., Chien, S., Skalak, R., 1988. Leukocyte relaxation properties, 54, 331-336.

Ting-Beall, H.P., Lee, A.S., Hochmuth, R.M., 1995. Effect of Cytochalasin D on the mechanical properties and morphology of passive human neutrophils. Annals of Biomedical Engineering 23, 666–671.

Tsai, M.A., Frank, R.S., Waugh, R.E., 1994. Passive mechanical behavior of human neutrophils: effect of cytochalasin B. Biophysical Journal 66, 2166–2172.

Wong, P.K., Wang, T.-H., Deval, J.H., Ho, C.-M., 2003. Electrokinetics in micro devices for biotechnology applications. IEEE/ASME Transactions on Mechatronics, in press.

Yao, W., Chen, K., Wang, X., Xie, L., Wen, Z., Yan, Z., Chien, S., 2002. Influence of TRAIL gene on biomechanical properties of the human leukemic cell line Jurkat. Journal of Biomechanics 35, 1659–1663.

Yarmola, E.G., Somasundaram, T., Boring, T.A., Spector, I., Bubb, M.R., 2000. Actin-latrunculin a structure and function. The Journal of Biological Chemistry 275, 28120–28127.

Zimmermann, U., 1982. Electric field-mediated fusion and related electrical phenomena. Bichimica et Biophysica Acta 694, 227–277.

Zimmermann, U., Friedrich, U., Mussauer, H., Gessner, P., Hämel, K., Sukhorukov, V., 2000. Electromanipulation of mammalian cells: Fundamentals and application. IEEE Transactions on Plasma Science 28, 72–82.